

Optimising geological mapping of glacial deposits using high-resolution electromagnetic induction data

Knud Erik S. Klint, Ingelise Møller, Pradip K. Maurya, and Anders V. Christiansen

There is a growing demand in modern society for detailed, localised geological maps and 3D models in connection with e.g. planning of major construction works, study of subsurface drainage systems, infiltration of storm water or risk assessment of contaminated waste dumps and pollution plumes. This demand is difficult to meet in Denmark as the surficial glacial deposits that cover most of the country are notoriously very heterogeneous. Standard geological maps are based on regional data collection, and their resolution is far from sufficient to identify structural elements on the 10–20 m scale needed in the above-mentioned applications.

Geophysical mapping for geological characterisation of the upper *c.* 5 m of the subsurface can be carried out using for instance direct-current geoelectrical methods (e.g. Loke *et al.* 2013), induced polarisation (e.g. Revil *et al.* 2012) set up with 1–2 m electrode spacing, electromagnetic induction (EMI; e.g. Christiansen *et al.* 2016; Doolittle & Brevik 2014), ground penetrating radar (GPR; e.g. Neal 2004) or seismic refraction tomography using a multicomponent landstreamer (e.g. Brodic *et al.* 2015). The resulting geophysical maps show the distribution of the measured parameter, for instance electric resistivity or seismic velocity. To construct *geological* maps using geophysical methods, the data must be verified and calibrated with geological field observations. GPR imaging of geological structures require laborious interpretation before a geological map can be constructed, and the method is limited to low-loss materials such as sandy sediments (Neal 2004).

A new approach, using a combination of shallow, high-resolution EMI surveying and traditional spear-auger soil sampling along the same transects, was tested in an area of *c.* 2 km² around the contaminated, former landfill site at Pillemark on Samsø (Fig. 1). The resistivity recorded using the EMI method is strongly related to the clay content, and this parameter is therefore well suited for geological mapping. The EMI method is also robust, data acquisition is 5–50 times faster than with other geophysical methods and the processing and inversion scheme is well defined (Christiansen *et al.* 2016).

Methodology

Spear-auger mapping

In the past almost 130 years, the geological mapping of the surficial cover of Denmark has largely been based on simple collection of pristine samples of the local sediment below the mull horizon using a specially designed sampling device, the so-called *spear auger*. This is a 1 m long steel rod with a diameter of 12 mm, a handle bar, and a 15–25 cm long, single or double slit at its tip. When the spear is pushed into the ground and turned, the slit captures a small soil sample (Fig. 2). The mapping geologist interprets the nature and origin of the sample and adds a soil-type symbol to a field map currently using the terminology described by Jakobsen *et al.* (2011). To map the boundaries between different soil types, samples are collected with a distance of 100–200 m depending on the local geological complexity. The symbols are then transferred to a master

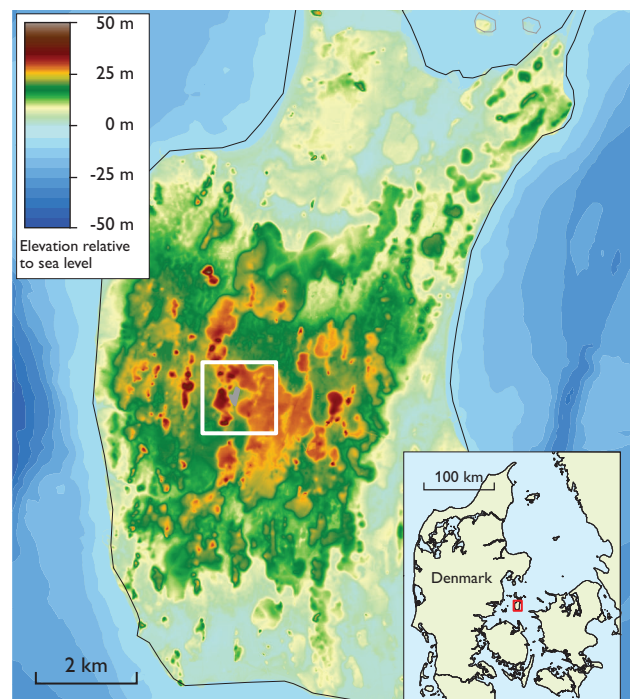


Fig. 1. The location of the study area on the island of Samsø is shown on the digital terrain model.



Fig. 2. Traditional geological mapping using the spear auger.

map sheet on a scale of 1:25 000; the resolution of the resulting geological map is about ± 100 m.

Geophysical mapping by electromagnetic induction

EMI methods are commonly used for soil mapping (e.g. Doolittle & Brevik 2014). During the last decade the development of multi-coil sensors, integration with GPS and use of inversion algorithms for data interpretation (e.g. Christiansen *et al.* 2016; Doolittle & Brevik 2014), have made EMI a very fast technique for mapping the resistivity of the upper 4–8 m of the subsurface (Fig. 3). The multi-coil DUALEM-421S sensor used in our study transmits an electromagnetic wave at 9 KHz from a horizontal coil and samples the total signal in horizontal and vertical receiver coils 1, 2 and 4 m from the transmitter coil. A signal is received $10 \times$ per second, making the equipment suitable for towing behind a motorised vehicle (Fig. 3).

Acquisition of field data in the study area

The EMI survey of the study area comprised *c.* 85 line-km mainly by towing; in difficult terrain and vegetation the sensor was carried manually. The EMI data were (1) averaged using a running mean filter of 2 m, (2) outliers manually culled and (3) inverted using a full-solution 1D algorithm (Auken *et al.* 2015), where the models are linked by 3D constraints to obtain a pseudo-3D resistivity model (Viezzoli *et al.* 2008). The resistivity models were discretised in 10 layers covering the upper 10 m of the subsurface; the mean depth of investigation was *c.* 6 m (Christiansen & Auken 2012). The interval resistivity at 1–2 m below



Fig. 3. The EMI survey system towed behind a vehicle. The *c.* 4 m long sensor is located inside a white tube on two sleds. The GPS sensor is mounted in the front of the tube above the transmitter coil. A data logger and a computer controlling the data acquisition are placed on the vehicle.

surface was calculated (Fig. 4) and used together with the spear-auger mapping.

The EMI survey was conducted prior to the spear-auger mapping, and the selection of soil sampling points was adjusted to the interval resistivity map so that areas with highly variable resistivity were mapped at a resolution of 10–20 m between the sampling points and areas with more homogeneous resistivity were mapped at a lower resolution. In Fig. 4 soil symbols and transitions of polygons with similar soil types based primarily on the spear-auger mapping are shown as an overlay on the geophysical mapping. The final interpretation of the soil type distribution is shown in Fig. 5, where it is seen that the soil type boundaries could be drawn with much higher accuracy than with traditional spear-auger mapping.

Results

The Pillemark study area (Fig. 1) has a hummocky topography. The geological map (Fig. 5) shows that a large variety of soil types is present. Clayey deposits such as clay till partly overlying meltwater clay dominates the hills, whereas sandier deposits such as sandy tills, meltwater sand/gravel occur along the fringes of the hills and on the highest hilltops. Extramarginal sand predominates in the low-lying areas, in the lowermost areas and in local depressions partly covered with postglacial sediments such as freshwater sand, clay and peat.

Based on the combined mapping techniques, the depositional history of the soil types could be outlined. The hills are interpreted to consist of mainly layered lacustrine deposits, which were overridden by a glacier that deposited tills and potentially deformed the lake sediments before

- Postglacial deposits**
- FG Freshwater gravel
- ▨ FS Freshwater sand
- ∨ FL Freshwater clay/silt
- ⊥ FT Freshwater peat
- ∇ FP Freshwater gyttja
- Late glacial deposits**
- TS Extramarginal freshwater sand
- Glacial deposits**
- △ ML Clay till
- ⊘ ML Sandy clay till
- ⊗ ML Gravelly clay till
- M MS Sandy till
- DG Meltwater gravel
- DS Meltwater coarse sand
- = DL Meltwater clay

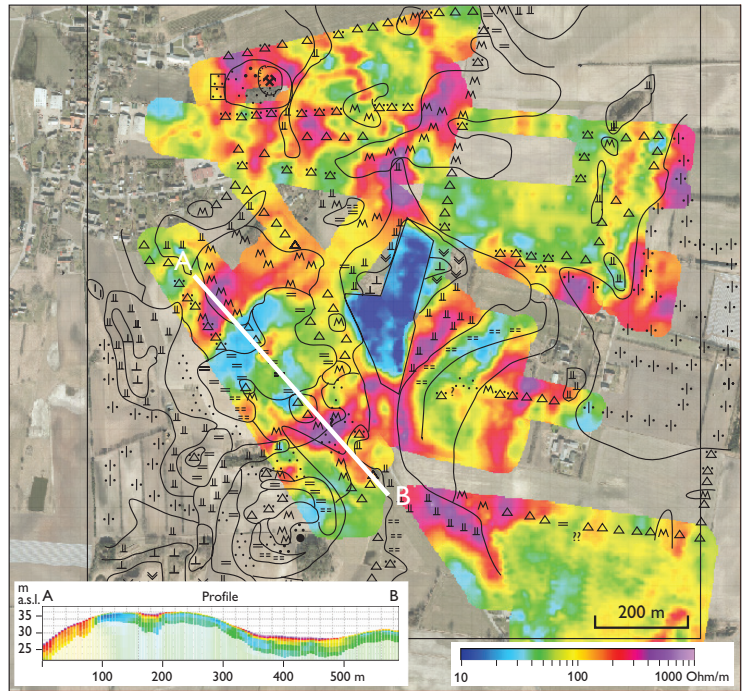


Fig. 4. Raw data from the spear-auger mapping and the interval resistivity at 1–2 m depth in the survey area. Note how the boundaries between soil types as interpreted in the field on this figure were modified during the construction of the geological map (Fig. 5). Note also the strong dark blue signature of the Pillemark landfill site, indicating the distribution of contaminated soil.

- Postglacial deposits**
- FS Freshwater sand
- FL Freshwater clay
- FT Freshwater peat
- Fill/town
- Late glacial deposits**
- TS Extramarginal freshwater sand
- Glacial deposits**
- DG Meltwater gravel
- DS Meltwater sand
- DL Meltwater clay
- MS Sandy till
- ML Clayey till

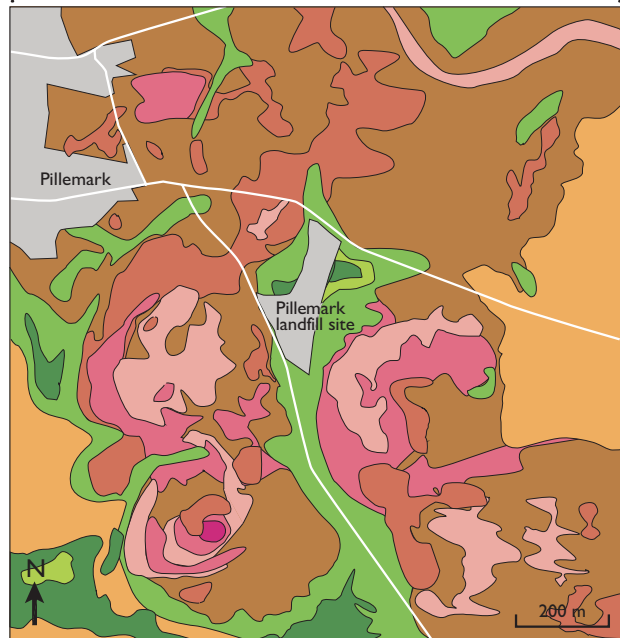


Fig. 5. High-resolution geological map of the research area based on combined spear-auger mapping and EMI surveying.

stagnating and melting. Lakes in local depressions were then slowly filled with postglacial freshwater sand, silt/clay and organic matter, slowly transforming into peat bogs. The landfill site was covered with anthropogenic soil and fill material; the outline of the contaminated soil is clearly apparent in Fig. 4.

Summary and perspectives

Compared to traditional spear-auger mapping, the combined EMI and spear-auger mapping makes it possible to produce high-resolution geological maps in highly heterogeneous glacial landscapes. It efficiently outlined the contaminated area at the landfill site. The method is considered solid and very cost-effective, since the total mapping of the area was carried out in three days plus another three days' work for processing the geophysical data and correlation with the spear-auger mapping.

Unfortunately, local disturbance from buried pipes, electrical wires etc. influences the quality of the geophysical data within a distance of 10–15 m from the instrument, making the technique less applicable in densely urbanised areas. Moreover, without using a GPS, the precision of spear-auger mapping is low on a 10-metre scale. A dedicated mapping exercise coordinating GPS positioning of all sampling points with geophysical measurements would increase the overall resolution. Finally, spear-auger mapping requires a well-trained geologist for interpreting the very small soil samples correctly.

The combined EMI and spear-auger mapping also has great potential for site characterisation, from general surveys on a scale of *c.* 10 km to local studies on a scale of *c.* 100 m. The methodology can easily be adapted to, or combined with, more dedicated soil sampling e.g. for detection of contaminated soil. There is also an obvious potential in other situations where high-resolution geological maps are needed, for example for identification of efficient infiltration areas in connection with establishment of suburban drainage systems (Bockhorn *et al.* 2015).

Acknowledgements

This study was supported by the research project GEOCON – advancing Geological, geophysical and Contaminant monitoring technologies for contaminated site investigation (contract 1305-00004B). Funding for this is provided by The Danish Council for Strategic Research under the Programme commission on sustainable energy and environment.

References

- Auken, E. *et al.* 2015: An overview of a highly versatile forward and stable inverse algorithm for airborne, ground-based and borehole electromagnetic and electric data. *Exploration Geophysics* **46**, 223–235, <http://dx.doi.org/10.1071/EG13097>
- Bockhorn, B., Klint, K.E.S., Jensen, M.B. & Møller, I. 2015: Use of geological mapping tools to improve the hydraulic performance of SuDS. *Water Science and Technology* **71**, 1492–1499, <http://dx.doi.org/10.2166/wst.2015.125>
- Brodic, B., Malehmir, A., Juhlin, C., Dynesius, L., Bastani, M. & Palm, H. 2015: Multicomponent broadband digital-based seismic land-streamer for near-surface applications. *Journal of Applied Geophysics* **123**, 227–241, <http://dx.doi.org/10.1016/j.jappgeo.2015.10.009>
- Christiansen, A.V., Pedersen, J.B., Auken, E., Søe, N.E., Holst, M.H. & Kristiansen, S.M. 2016: Improved geoarchaeological mapping with electromagnetic induction instruments from dedicated processing and inversion. *Remote Sensing* **8**, 1022, <http://dx.doi.org/10.3390/rs8121022>
- Christiansen, A.V. & Auken, E. 2012: A global measure for depth of investigation. *Geophysics* **77**, WB171–177, <http://dx.doi.org/10.1190/geo2011-0393.1>
- Doolittle, J.A. & Brevik, E.C. 2014: The use of electromagnetic induction techniques in soils studies. *Geoderma* **223–225**, 33–45, <http://dx.doi.org/10.1016/j.geoderma.2014.01.027>
- Jakobsen, P.R., Hermansen, B. & Tougaard, L. 2011: Danmarks digitale jordartskort 1:25 000 Version 3.1. Danmarks og Grønlands Geologiske Undersøgelse Rapport **2011/40**. Copenhagen: Geological Survey of Denmark and Greenland.
- Loke, M.H., Chambers, J.E., Rucker, D.F., Kuras, O. & Wilkinson, P.B. 2013: Recent developments in the direct-current geoelectrical imaging method. *Journal of Applied Geophysics* **95**, 135–156, <http://dx.doi.org/10.1016/j.jappgeo.2013.02.017>
- Neal, A. 2004: Ground-penetrating radar and its use in sedimentology: Principles, problems and progress. *Earth-Science Review* **66**, 261–330, <http://dx.doi.org/10.1016/j.earscirev.2004.01.004>
- Revil, A., Karaoulis, M., Johnson, T. & Kemna, A. 2012: Review: Some low-frequency electrical methods for subsurface characterization and monitoring in hydrogeology. *Hydrogeology Journal* **20**, 617–658, <http://dx.doi.org/10.1007/s10040-011-0819-x>
- Viezzoli, A., Christiansen, A.V., Auken, E. & Sørensen, K. 2008: Quasi-3D modeling of airborne TEM data by spatially constrained inversion. *Geophysics* **73**, F105–113, <http://dx.doi.org/10.1190/1.2895521>

Authors' addresses

K.E.S.K., *GEO, Maglebjergvej 1, DK-2800 Kgs. Lyngby, Denmark*; E-mail kek@geo.dk.

I.M., *Geological Survey of Denmark and Greenland (GEUS), Øster Voldgade 10, DK-1350 Copenhagen K, Denmark*

P.K.M & A.V.C., *Hydrogeophysics Group, Department of Geoscience, Aarhus University, C.F. Møllers Allé 4, DK-8000 Aarhus C, Denmark.*